

INTERNATIONAL UNION OF PURE AND APPLIED CHEMISTRY

MACROMOLECULAR DIVISION
COMMISSION ON POLYMER CHARACTERIZATION AND PROPERTIES
WORKING PARTY ON STRUCTURE AND PROPERTIES
OF COMMERCIAL POLYMERS*

Intrinsic Characterization of Continuous Fibre
Reinforced Thermoplastic Composites—III

A COLLABORATIVE STUDY OF THE STRUCTURE AND MORPHOLOGY IN CONTINUOUS FIBER REINFORCED PET AND PEEK

(Technical Report)

Prepared for publication by

J. C. SEFERIS¹, D. R. MOORE² and H. G. ZACHMANN³

¹Polymeric Composites Laboratory, Department of Chemical Engineering, BF-10,
University of Washington, Seattle, Washington 98195, USA

²ICI Research Centre, POB 90, Wilton, Middlesbrough, Cleveland TS6 8JE, UK

³Institute für Technische und Makromolekulare Chemie der Universität,
University of Hamburg, FRG.

*Membership of the Working Party during 1991–93 is as follows:

Chairman: D. R. Moore (UK); *Secretary:* H. M. Laun (FRG); *Members:* G. Ajroldi (Italy); P. S. Allan (UK); R. S. Bailey (UK); M. Bevis (UK); C. B. Bucknall (UK); M. Cakmak (USA); A. Cervenka (UK); D. Constantin (France); J. Curry (USA); M. C. Dehennau (Belgium); M. J. Doyle (USA); M. Fleissner (FRG); A. Ghijssels (Belgium); Y. Giraud (France); L. Glas (Netherlands); W. Gleissle (FRG); A. Gray (UK); D. J. Groves (UK); B. Gunesin (USA); J. Hoeymans (Belgium); P. S. Hope (UK); T. A. Huang (USA); M. Kozlowski (Poland); J. Lyngaae-Jorgensen (Denmark); F. H. J. Maurer (Netherlands); A. P. Plochocki (USA); S. Röber (FRG); J. C. Seferis (USA); J. Stejskal (Czechoslovakia); S. S. Sternstein (USA); P. Szewczyk (Poland); S. Turner (UK); G. Vassilatou (USA); T. Vu-Khanh (Canada); J. L. White (USA); H. G. Zachmann (FRG).

Names of countries given after Members' names are in accordance with the *IUPAC Handbook 1991–1993*; changes will be effected in the 1993–95 edition.

Republication of this report is permitted without the need for formal IUPAC permission on condition that an acknowledgement, with full reference together with IUPAC copyright symbol (© 1993 IUPAC), is printed. Publication of a translation into another language is subject to the additional condition of prior approval from the relevant IUPAC National Adhering Organization.

A collaborative study of the structure and morphology in continuous fiber reinforced PET and PEEK (Technical Report)

Abstract

The WAXS pattern of the continuous carbon fiber reinforced laminates can be viewed as a superposition of the scattering patterns arising from the carbon fibers and the polymer matrix. In order to obtain the scattering of the matrix alone, the scattering of the pure reinforcing fibers has been measured at different azimuthal angles. A procedure has been developed to subtract the scattering of the fibers from that of the complete laminate. From the corrected scattering diagrams, the degree of crystallinity has been determined. Both PET and PEEK based laminates were examined in this study, and crystalline fractions of $x_C = 0.46$ and $x_C = 0.34$ were determined for the PET and PEEK matrix composites, respectively. These values are in good agreement with the results obtained from calorimetric measurements.

In addition, for laminates laid-up in a $\pm 45^\circ$ configuration, it was determined that the actual layup angle was $\pm 42.6^\circ$ in the PET laminates, whereas the layup angle was measured to be exactly $\pm 45^\circ$ in the PEEK composite. These results illustrate that small variations in layup configurations can be detected by the developed procedures.

Pole figures obtained from the PEEK laminates indicated that there was no overall orientation of the matrix. Thus, the pole figures were completely determined by the orientation of the carbon fibers in the laminate and the orientation of the crystals within the carbon fibers.

INTRODUCTION

Thermoplastics are becoming an interesting alternative to epoxies in applications as matrix materials in high performance composites. As the bulk properties of all composites are highly dependent on the properties of the matrix reinforcement material, it is of great interest to find methods for determining the structure of the thermoplastic matrix. Most important is the determination of the degree of crystallinity and the orientation of the molecules. There exist several publications on composite matrix structure investigation by DSC and microscopy and citations may be found in references 1-4. However, only a few attempts have been made to investigate the structure through the use of X-ray scattering (5,6).

The aim of this investigation is to find methods to determine the degree of crystallinity and the molecular orientation in continuous carbon fiber reinforced poly(ethylene terephthalate) (CF/PET) and poly(ether-ether-ketone) (CF/PEEK) laminates, and to perform the corresponding measurements on the materials supplied by the IUPAC working party. The materials investigated are a $\pm 45^\circ$ laminate of CF/PET and a $\pm 45^\circ$ laminate of CF/PEEK.

Although PET does not seem to be a promising material for use in high performance thermoplastic applications, it was chosen for this investigation as a reference material because its crystallization and orientation behavior has been well investigated (7-9). PEEK, on the other hand, is a higher performance thermoplastic resin, and has already been successfully used as a matrix in composites. Its continuous carbon fiber reinforced laminates show very good mechanical properties (10,11) and already some studies of neat PEEK crystallization behavior have been performed (3,12-14).

Investigations were performed at the following places:

1. University of Washington: Sample preparation
2. University of Akron: DSC measurements and WAXS
3. University of Hamburg: WAXS and pole figures

EXPERIMENTAL

Composite laminates in the $\pm 45^\circ$ configuration were laid-up and autoclaved following processing procedures described elsewhere (11).

The samples for DSC measurements were cut with a hand saw into circular shapes with weights ranging from 10 to 20 mg. The DSC scans were measured at a heating rate of $20^\circ\text{C}/\text{min}$ in a dry nitrogen atmosphere using a DuPont 912 Differential Scanning Calorimeter interfaced to a Dupont 9900 controller.

Wide angle X-ray scattering (WAXS) patterns were recorded on photographic films using a General Electric Generator operating at 40 kV and 20 mA, equipped with a copper target tube and a Furnas WAXS/SAXS combination camera. The X-rays were monochromatized by a Nickel foil filter to remove $\text{CuK}\beta$ radiation from the main beam. The samples were mounted so that the X-ray beam was normal to the surface of the composite.

WAXS diffractometry experiments were performed using a Siemens D500 diffractometer with a copper target tube. Data in both reflection and transmission modes were obtained. Again, a Nickel foil filter was used to remove the $\text{CuK}\beta$ radiation. For some of the experiments, a Rigaku Rotating anode (copper target) generator equipped with a horizontal diffractometer was used with the generator operating at 45 kV and 150 mA. For these cases, the X-ray beam was monochromatized by a graphite crystal monochromator located at the scanning arm.

X-Ray and DSC experiments were performed at four different locations on the composite laminate plaques. On each plaque, the samples were numbered 1 through 4, and their locations are shown schematically in Fig. 1.

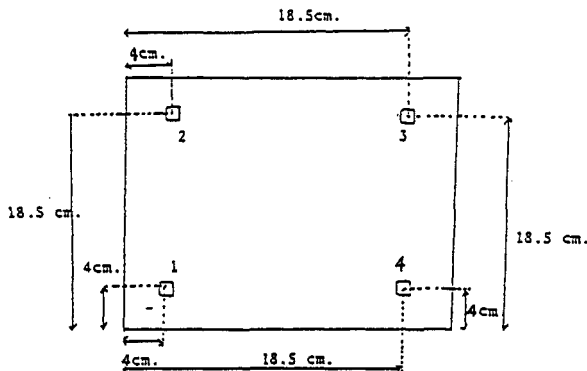


Fig. 1. Location of sample 1 to sample 4 on the CF/PET plaque and on the CF/PEEK plaque.

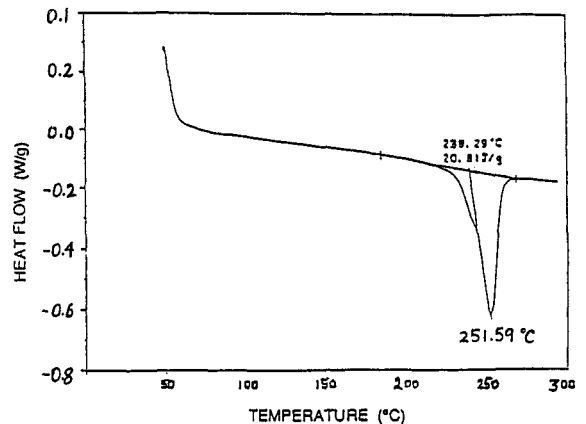


Fig. 2. DSC scan of CF/PET sample 1.

RESULTS ON CF/PET

1. Differential scanning calorimetry (DSC)

The DSC scan obtained from a CF/PET sample is shown in Fig. 2. The typical cold crystallization peak, normally observed in amorphous PET in the range of $130\text{--}150^\circ\text{C}$, is absent. Instead, two endothermic peaks are observed, a main peak at 250°C and a shoulder at 240°C . This behavior is typical of highly crystallized PET. Similar results were obtained for all of the PET samples examined, irrespective of location and results are summarized in Table 1.

TABLE 1. Melting temperature (position of the peak) T_m and enthalpy of fusion ΔH_f of the CF/PET composite

	T_m (°C)		ΔH_f (J/g)
	Primary	Secondary	
Location 1	252	240	20.8
Location 2	253	246	22.8
Location 3	254	247	22.0
Location 4	253	246	20.7

TABLE 2. Position of WAXS peaks of CF/PET composite (in transmission mode)

Peak	2θ
1	16.28
2	17.59
3	22.55
4	26.05
5	32.53
6	43

In order to calculate the degree of crystallinity from the measured enthalpy of fusion, it was necessary to determine the weight fraction of carbon fiber in the composite. This was done by dissolving the PET in tetrachloroethane/phenol. The amount of carbon fiber was determined to be 63.8% by weight. Using the average measured enthalpy of 21 J/g and assuming a theoretical melting enthalpy of 140 ± 20 J/g for 100% crystallized neat PET (15), the degree of crystallinity was calculated to be $42 \pm 7\%$. This is in good agreement with the results from X-ray analysis (see next section).

2. Wide angle x-ray scattering (WAXS)

(a) Overview of scattering patterns

The WAXS patterns obtained on locations 1 and 2 for the CF/PET sample are shown in Fig. 3. These patterns are a composite overlap of carbon fiber diffraction as well as PET diffraction. They do not indicate any appreciable orientation of the PET matrix. The "cross" pattern results from the $0/90^\circ$ layout of the carbon fibers.

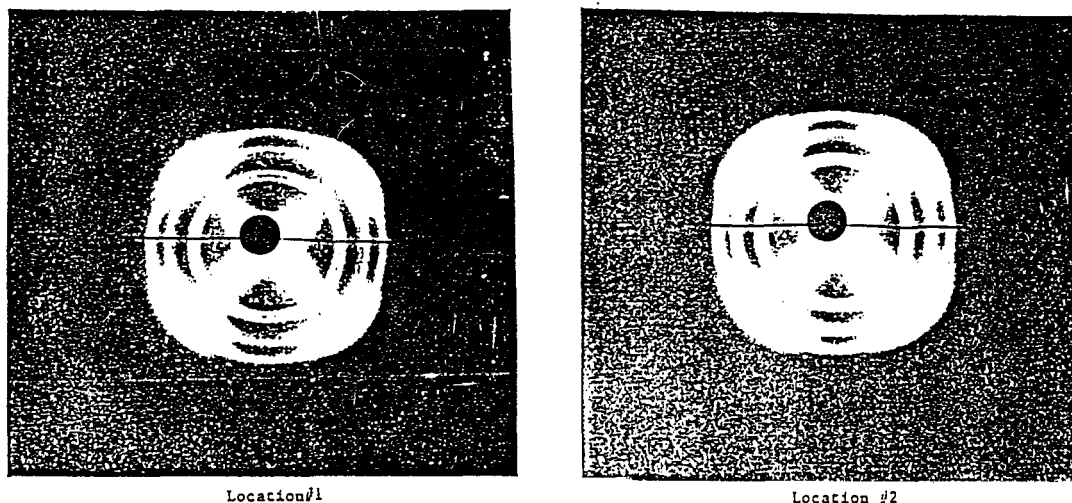


Fig. 3. WAXS pattern of CF/PET samples 1 and 2.

Transmission and reflection WAXS diffractometer scans were also performed on the sample to determine possible orientation in the PET matrix. A rectangular sample was cut from location 1 so that the vertical axis of the sample made a 45° angle with the carbon fibers, thereby minimizing the diffraction coming from the carbon fibers. The two diffractometer scans are shown in the Fig. 4. They indicate that the intensity of the diffraction in the reflection mode was much higher than in the transmission mode. This may be due to the strong absorption of X-rays in the transmission mode. It also appears that diffraction from the carbon fibers is more prevalent in the reflection diffractogram, whereas the transmission diffractogram mainly shows the PET peaks. Therefore, all measurements for quantitative evaluation reported in the following sections were performed in the transmission mode.

Finally, the angular positions of the crystal reflections in the CF/PET diffractometer scan were determined and are summarized in Table 2. The results are in complete agreement with reported values for unreinforced PET (16).

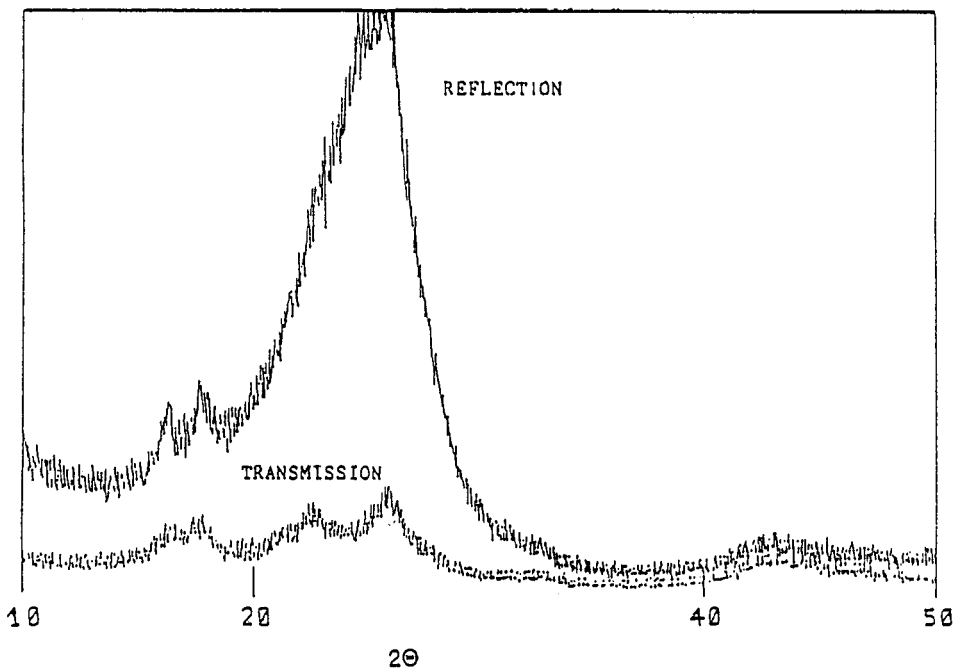


Fig. 4. WAXS of CF/PET sample 1 in reflection mode and in transmission mode.

(b) Quantitative studies

In order to separate the WAXS scattering of the carbon fiber from that of the PET and PEEK matrix, the scattering of a bundle of single carbon fibers was measured. Fig. 5 shows this scattering intensity as a function of scattering angle 2θ obtained at different azimuthal angles ϕ with respect to the normal of the carbon fiber axis. If $\phi = 0^\circ$, a scattering peak at $2\theta = 26^\circ$ appears; if $\phi = 90^\circ$, a scattering peak at $2\theta = 46^\circ$ is present. In addition, a strong increase in scattering intensity at small scattering angles can be observed for all values of the azimuthal angle ϕ .

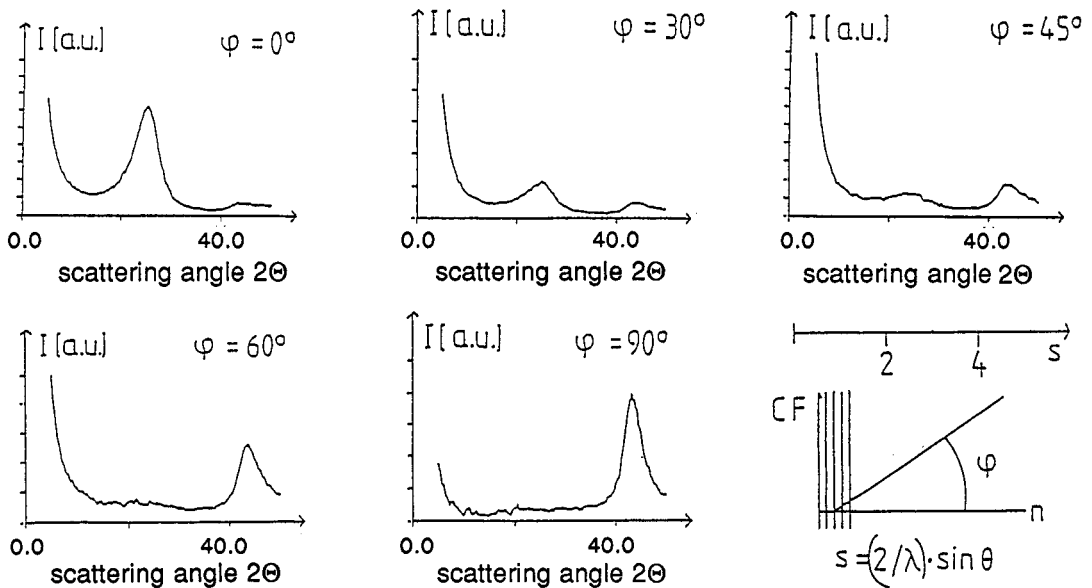


Fig. 5. WAXS of carbon fibers as a function of the scattering angle 2θ for five different values of the azimuthal angle ϕ .

For the determination of the scattering of neat PET, an unoriented sample was examined since no matrix orientation was observed in the scattering experiments with the PET composites. Fig. 6 shows the scattering diagram from an unoriented PET film that was annealed at 250°C for 3 hours, which corresponds approximately to the heat treatment of the processed laminates.

By comparing the scattering patterns of the carbon fibers and the neat PET (Figs. 5 and 6), it can be seen that the interference between the two scattering patterns is smallest at $\phi = 90^\circ$. However, since the samples examined in this study were all made with a $\pm 45^\circ$ laminate configuration, no data could be generated where all the fibers would have been at an azimuthal angle of $\phi = 90^\circ$. Thus, the best alternative for minimizing the interference for a $\pm 45^\circ$ laminate is at an azimuthal angle $\phi = 45^\circ$, and this is the angle where all of the WAXS patterns were analyzed for the composite.

In order to determine the exact orientation of the fibers in the $\pm 45^\circ$ CF/PET laminate, the scattering was measured at the fixed scattering angle $2\Theta = 25.9^\circ$, corresponding to the peak of the carbon fibers, while the sample was rotated with respect to the laminate plane. The result is shown in Fig. 7. For the $\pm 45^\circ$ laminate, the maxima are expected to be separated by a constant value $\Delta\phi = 90^\circ$. However, the figure shows that the distances were not equal. A periodic angle difference of $\Delta\phi = 85.2^\circ$ followed by a $\Delta\phi = 94.8^\circ$ was observed, which implies that the sample is actually a $\pm 42.6^\circ$ laminate.

Fig. 8 shows the scattering diagram of this laminate measured at the azimuthal angle $\phi = 42.6^\circ$, which corresponds to the lamination angle. As previously discussed, at this value of ϕ , the scattering intensity of the carbon fiber at $2\Theta = 25.9^\circ$ should be at a minimum for this laminate configuration. In this figure, the scattering intensity is plotted as a function of the scattering vector s , which is defined as $s = (2/\lambda) \sin 2\Theta$, where λ is the wavelength of the radiation used (1.54 Å for $\text{CuK}\alpha$), and 2Θ is the scattering angle. As can be seen, there is residual scattering from the carbon fibers at $s = 2.9 \text{ nm}^{-1}$ (corresponding to $2\Theta = 25.9^\circ$) and in the region of small values of 2Θ . The scattering of the carbon fibers measured at $\phi = 42.6^\circ$ was multiplied by a constant factor derived by fitting it to the scattering curve of the composite at small scattering angles. The fitted curve was then subtracted from the scattering curve of the composite. The result is shown in Fig. 9. Good agreement between this curve and that generated for the neat PET sample shown in Fig. 6 was observed. This proves that the correction performed with respect to the carbon fiber is appropriate.

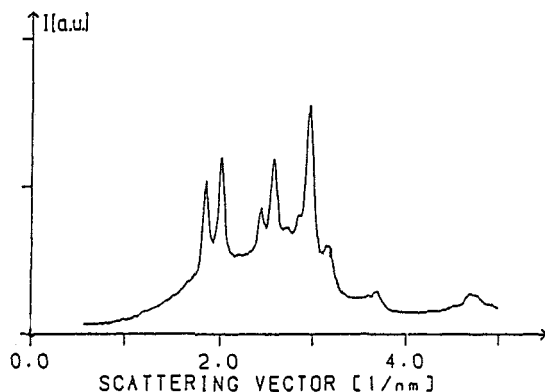


Fig. 6. WAXS of annealed PET as a function of the scattering vector s .

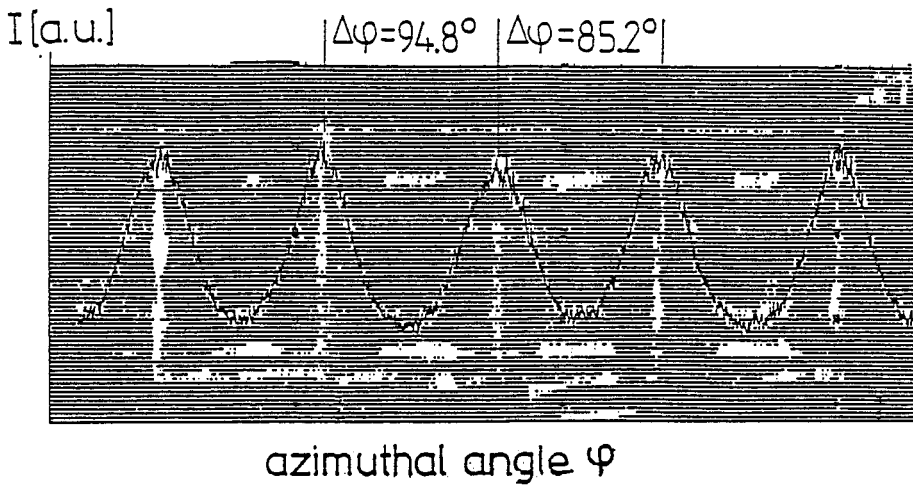


Fig. 7. WAXS of CF/PET at $2\theta = 25.9^\circ$ as a function of the azimuthal angle ϕ .

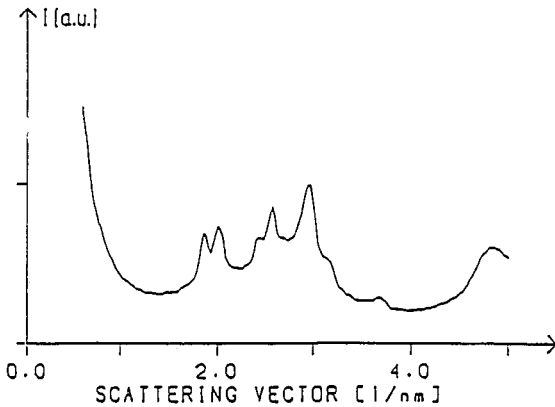


Fig. 8. WAXS of CF/PET as a function of the scattering vector s .

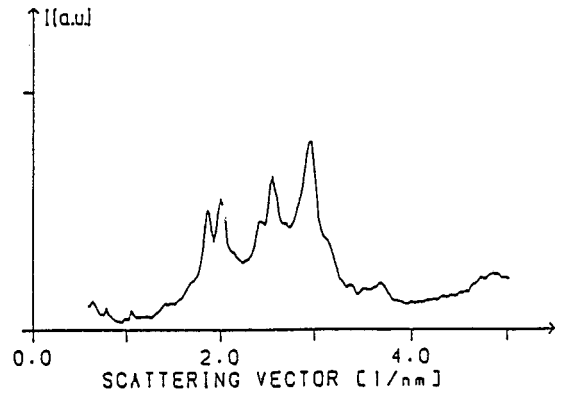


Fig. 9. WAXS of CF/PET as a function of the scattering vector s after subtraction of the WAXS of the carbon fiber.

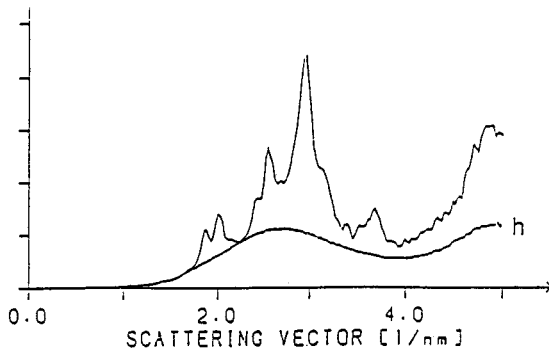


Fig. 10. WAXS intensity multiplied by s^2 as a function of the scattering vector s of PET in the CF/PET sample and of the amorphous halo h .

Finally, the extracted data, free from carbon fiber scattering, were used to evaluate the degree of crystallinity in the PET matrix. The amorphous halo, as measured with a neat amorphous PET sample, was fitted to the curve in Fig. 9 after corrections for air scattering and Compton scattering were performed (17). The results are shown in Fig. 10. The degree of crystallinity was determined as the fraction of scattered intensity lying above the amorphous halo integrated from $s = 0$ to $s = 4.22 \text{ nm}^{-1}$. Within this region, the total integrated scattering intensity was found to be independent of the state of order (17). A value of $x_c = 0.46$ was found, which is in good agreement with the DSC result.

RESULTS ON CF/PEEK

1. Differential scanning calorimetry (DSC)

The DSC curve obtained from sample 1 of the CF/PEEK is shown in Fig. 11. No cold crystallization peak was observed in the temperature range from 150° to 200°C, which indicates that the level of crystallinity of the PEEK matrix in the laminate was relatively observed both in neat PEEK and in PEEK composites and have been discussed elsewhere (18,19). The glass transition temperature (T_g) was at 153.8°C and the total heat of fusion from the composite was 17.0 J/g. Similar results were observed for the other three samples.

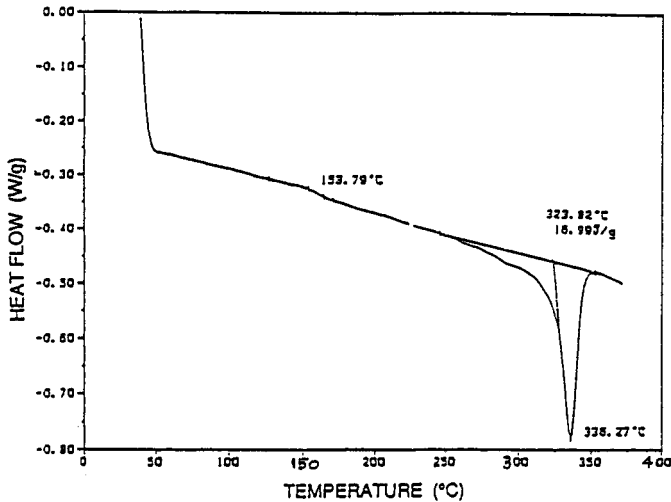


Fig. 11. DSC scan of CF/PEEK sample 1.

TABLE 3. Position of WAXS peaks of CF/PEEK

Peak	2θ
1	18.8
2	20.95
3	23.1
4	25.3
5	28.85
6	32.8

2. Wide angle x-ray scattering (WAXS)

(a) Overview of scattering patterns

Similar to PET, wide angle X-ray diffraction (WAXS) experiments were performed using both flat film and diffractometry techniques. The WAXS film patterns showed uniform azimuthal intensity distribution in each crystal reflection circle. This indicates the absence of orientation in the PEEK matrix.

Wide angle X-ray diffractometer scans were obtained for all four positions in the reflection mode using the Rigaku Denki 12 kW rotating copper anode generator. The data on all four positions for both smooth surface and rough surface facing the X-ray beam are given in Fig. 12. For clarity, each scan was off-set by 1 kHz in the y-axis in this figure. There were no apparent variations between the sample locations.

A comparison of the diagrams obtained in transmission and in reflection is shown in Fig. 13. Again as with the CF/PET laminate, the scattering of the carbon fiber is much stronger in the reflection mode than it is in the transmission mode.

The positions of the crystalline peaks of CF/PEEK are listed in Table 3. They agree with the results obtained for neat PEEK (1).

(b) Quantitative studies

Quantitative evaluation of the wide angle X-ray scattering of the $\pm 45^\circ$ CF/PEEK laminate was performed similarly to that of the CF/PET laminate.

Fig. 14 shows the scattering diagram of the fiber reinforced $\pm 45^\circ$ laminate measured at an azimuthal angle $\phi = 45^\circ$ with respect to the fibers. Fig. 15 shows the dependence of scattered intensity at vector $s = 2.9 \text{ nm}^{-1}$ (at $2\theta = 25.9^\circ$) during rotation of the sample

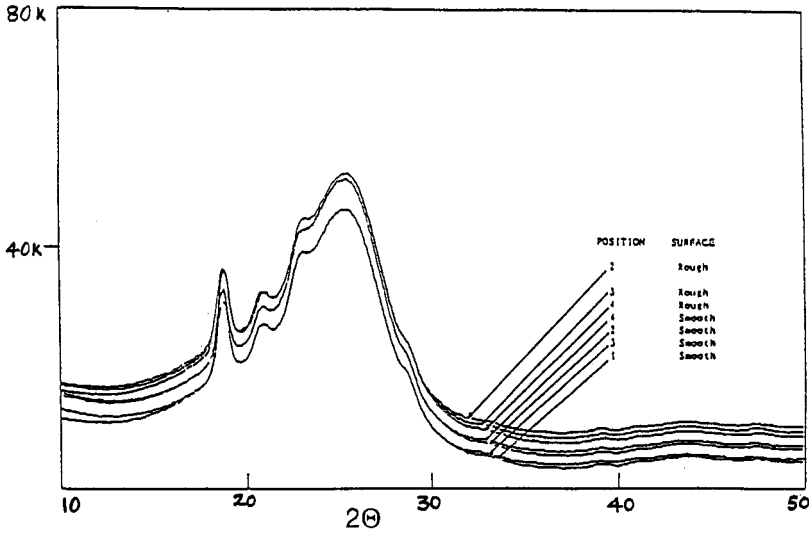


Fig. 12. WAXS of CF/PEEK samples 1 through 4 in transmission.

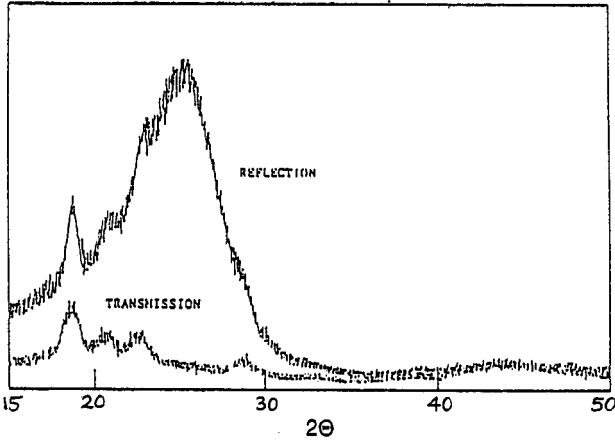


Fig. 13. WAXS of CF/PEEK sample 1 in transmission mode and in reflection mode.

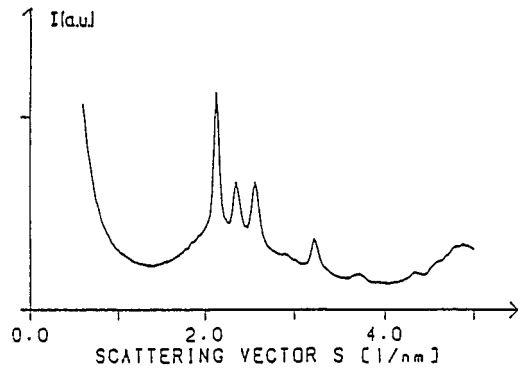


Fig. 14. WAXS of CF/PEEK as a function of the scattering vector s .

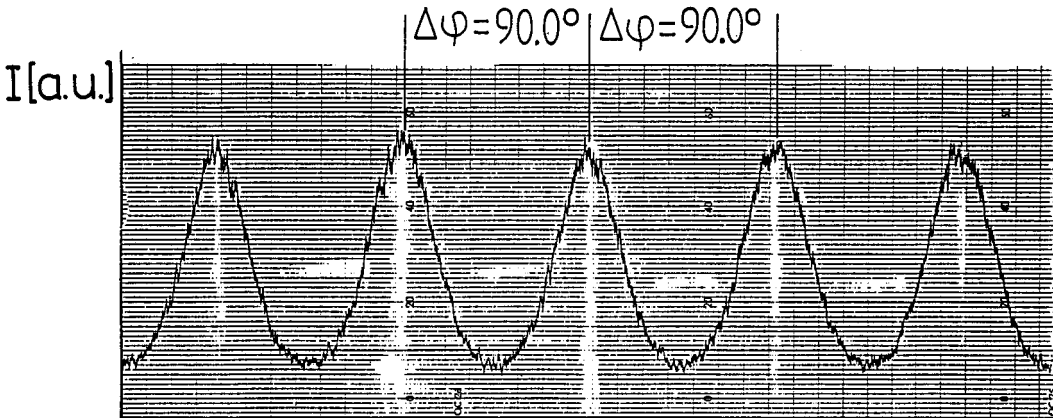


Fig. 15. WAXS of CF/PEEK at $2\theta = 25.9^\circ$ as a function of the azimuthal angle ϕ .

as a function of ϕ . In contrast to the results of the CF/PET sample, the distance between adjacent peaks is exactly 90° . This proves that the fibers have the exact orientation corresponding to a $\pm 45^\circ$ laminate.

Fig. 16 illustrates the results obtained by subtracting the scattering of the carbon fiber from that of the carbon fiber reinforced PEEK. For comparison, the corresponding diffraction diagram of a crystalline PEEK sample without fibers is shown in Fig. 17.

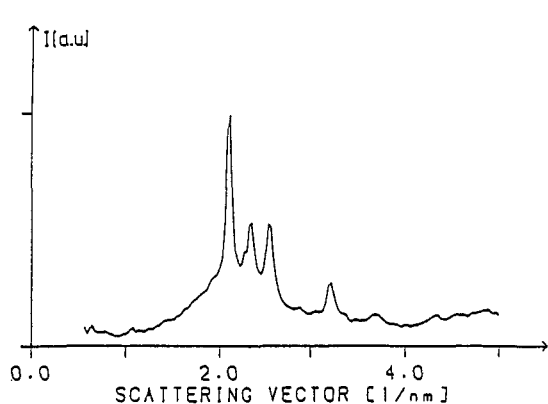


Fig. 16. WAXS of CF/PEEK as a function of the scattering vector s after subtraction of the WAXS of the carbon fiber.

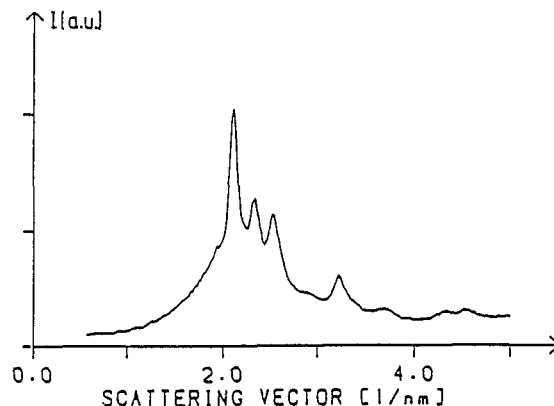


Fig. 17. WAXS of annealed PEEK as a function of the scattering vector s .

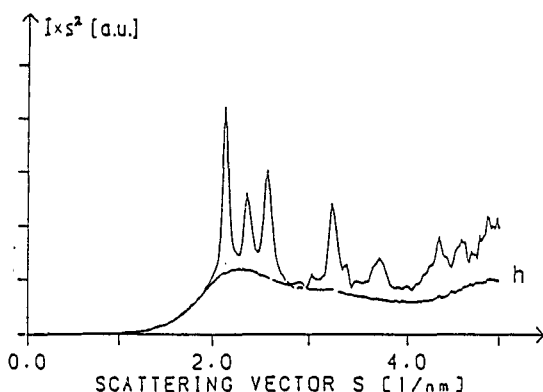


Fig. 18. WAXS intensity multiplied by s^2 as a function of the scattering vector s of PEEK in the sample of CF/PEEK and of the amorphous halo h .

Finally, Fig. 18 represents the corrected scattering curve of the laminate together with the amorphous halo of PEEK. By evaluating the region between $s = 0$ and $s = 4.1 \text{ nm}^{-1}$, a degree of crystallinity $x_c = 0.34$ was obtained.

3. Pole figures

In addition to the scattering diagram, pole figures were measured at the scattering angles corresponding to the four strongest peaks of PEEK (Figs. 19 and 20). At all four scattering angles, the same type of orientation distribution is obtained. This indicates that on the average, PEEK is unoriented, and the dependence of the scattered intensity on the direction of the incident beam with respect to the sample is caused by the orientation of the carbon fibers. Thus, the pole figures represent the orientation distribution of the carbon fibers superimposed with the orientation distribution of the graphite crystals within each fiber.

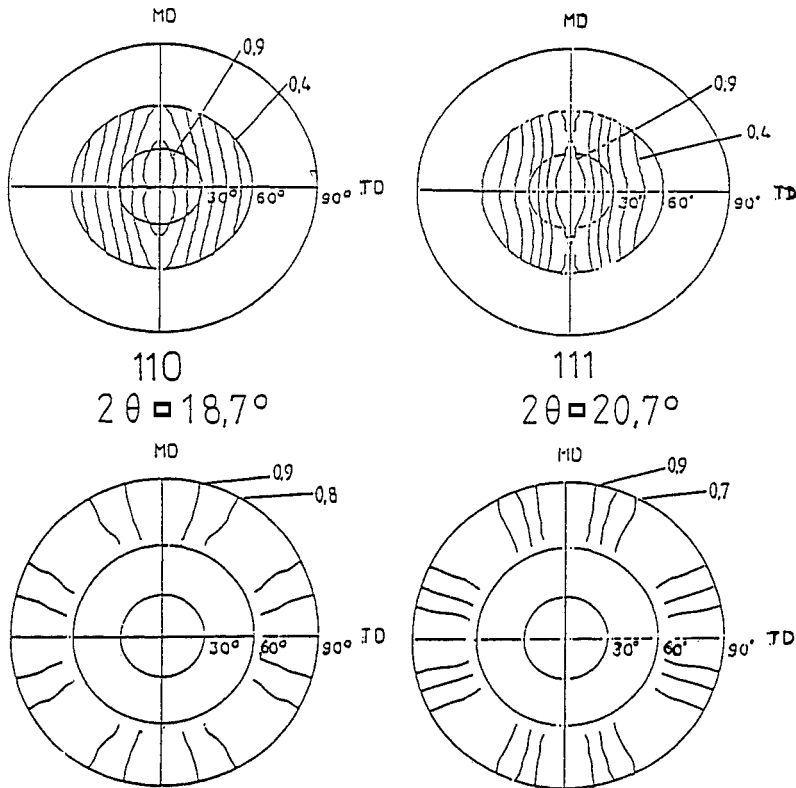


Fig. 19. Pole figure of CF/PET at different values of 2θ as measured in reflection (top) and transmission (bottom).

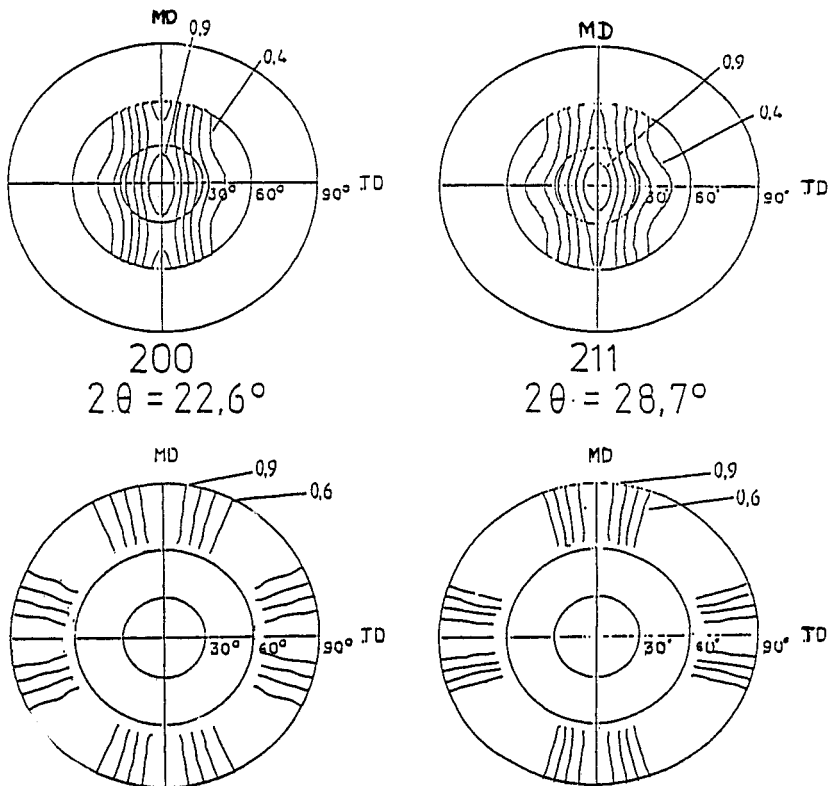


Fig. 20. Pole figure of CF/PEEK at different values of 2θ as measured in reflection (top) and transmission (bottom).

In the case of transmission measurements, there are two preferred orientations, which coincide with the two directions of fiber orientation in the laminate, designated by "MD" and "TD". However, with reflection measurements, only one preferred orientation, coinciding with the direction of the fibers in the surface layer of the laminate, is obtained. The perpendicular fibers, which are lying in the inner layers of the laminate, only cause a slight deformation of the pole figure. This is due to the absorption of the X-rays. According to this effect, in reflection the main contribution of the scattering arises from the upper layer of the laminate, whereas in the transmission mode, all layers contribute to the same extent. This is confirmed by the following estimation.

The average absorption coefficient of a CF reinforced PEEK laminate of the same composition as the one investigated in this work is $\mu = 8.79 \text{ cm}^{-1}$. The thickness of the first layer in the laminate is $t = 0.015 \text{ cm}$. In reflection measurements at $2\Theta = 22.6^\circ$, the X-rays pass this layer twice through an angle lying between 11.3° and 5.6° which corresponds to an actual path length d of between 0.155 cm and 0.31 cm . By this effect, the intensity scattered by the inner layer is reduced according to $I/I_0 = \exp(-\mu t)$ which corresponds to a value of between 0.26 and 0.066 . Consequently, the scattering observed in reflection may be attributed mainly to the surface.

According to the microscopic investigations, the carbon fibers act as a nucleating agent for crystallization, causing some oriented crystal growth. Since we have cylindrical symmetry around each fiber and two directions of fibers are mutually perpendicular, then the averaging over a larger part of the sample that occurs during the X-ray scattering experiment results in isotropic scattering.

CONCLUSIONS

The results show that wide angle X-ray scattering can be used to determine:

1. The degree of crystallinity of the thermoplastic matrix
2. The orientation distribution of the fibers

In further investigations one can try to improve the method of subtraction of the carbon fiber by performing measurements on the composite at two different azimuthal angles. By subtraction of the two scattering diagrams, the scattering of the matrix is eliminated and the absolute intensity of the scattering of the pure fibers can be obtained.

By means of this procedure, a method to obtain the amount of fibers in the composite by WAXS would also be available. Such a method would be very useful in those cases where the matrix cannot be as easily dissolved as PET. Once the exact amount of fibers is determined, additional measurements of the degree of crystallinity could be performed by DSC and density techniques.

There also exists the possibility to determine the amount of fiber by X-ray absorption measurements. These measurements were beyond the scope of this collaborative study, but were performed and are discussed in a separate publication by Schipp, Röber, Zachmann, and Seferis (20).

Additionally, if a composite is available in which fiber alignment is perfect, pole figures can be used to determine the orientation distribution of the graphite crystals within the fibers. Alternatively, if the orientation distribution of the crystals within a fiber is known, then the orientation of the fibers in an imperfectly aligned composite can then be determined.

Acknowledgement

The authors would like to express their appreciation to S. Röber and U. Köncke of the University of Hamburg and J. Ferrara and K. Nelson of the University of Washington for performing the measurements and data analysis and for discussions concerning this work.

REFERENCES

1. D. J. Blundell and B. N. Osborn, *Polymer*, **24**, 953 (1983).
2. Y. Lee and R. S. Porter, *Poly. Eng. Sci.*, **26**, 9 (1986).
3. C. N. Velisaris and J. C. Seferis, *Poly. Eng. Sci.*, **26**, 22 (1986).
4. J. C. Seferis, C. Allstrom, and S. Dillman, Proc. SPE ANTEC '87, 1467 (1987).
5. T. C. Hsu and P. H. Geil, *J. Mat. Sci.*, **24**, 4 (1989).
6. K. M. Nelson, J. C. Seferis, and H. G. Zachmann, *J. Appl. Poly. Sci.*, **42**, 1289 (1991).
7. H. G. Zachmann and H. A. Stuart, *Makromol. Chemie.*, **49**, 131 (1960).
8. B. Günther and H. G. Zachmann, *Polymer*, **24**, 1008 (1983).
9. T. Ozawa, *Polymer*, **12**, 150 (1971).
10. J. C. Seferis, *Polymer Composites*, **7**, 3 (1986).
11. D. R. Moore and J. C. Seferis, *Pure Applied Chemistry*, in Preparation.
12. W. I. Lee and G. S. Springer, *J. Comp. Mat.*, **21**, 1054 (1987).
13. M. A. Grayson and C. J. Wolf, *Poly. Mat. Sci. Eng.*, **58**, 514 (1988).
14. P. Cebe, *Poly. Eng. Sci.*, **28**, 18 (1988).
15. B. Wunderlich, "Macromolecular Physics," Vol. 3, Academic Press, New York, 1976.
16. C. W. Bunn and R. de P. Danbury, *Trans. Faraday Soc.*, **50**, 1173 (1954).
17. R. Gehrke and H. G. Zachmann, *Makromol. Chemie.*, **182**, 627 (1981).
18. G. M.K. Osterberg and J. C. Seferis, *J. Appl. Poly. Sci.*, **33**, 29 (1987).
19. Y. Lee and R. S. Porter, *Macromolecules*, **20**, 1336 (1987).
20. C. Schipp, S. Röber, H. G. Zachmann, and J. C. Seferis, *J. Poly Sci. (Phys. Ed.)*, in Preparation.